Search for Non-Standard Model Physics in Rare Decays at the Tevatron

G. Volpi[a] on behalf of CDF and DØ collaborations

[a]Univ and INFN Pisa, L.go Bruno Pontecorvo 3, 56127 Pisa, Italy

In this proceeding we report the most recent results from the CDF and DØ collaborations on the rare decays of b-mesons. The presented results involve show a new DØ limit for $\mathcal{B}\left(B_s^0 \to \mu^+\mu^-\right)$ that represent the best single measurement on this mode so far, the updates of the $\mathcal{B}\left(B_s^0 \to \phi\phi\right)$ with for the first time an angular analysis on the final state, a new measurement of the $\mathcal{B}\left(B^0 \to K^{\star 0}\mu^+\mu^-\right)$ and $\mathcal{B}\left(B^+ \to K^+\mu^+\mu^-\right)$ with an interesting measurement on the forward-backward asymmetry for those channels and the first observation of the $\mathcal{B}\left(B_s^0 \to \phi\mu^+\mu^-\right)$.

1. Introduction

The search for the rare b-hadron decays is an important precision test for the Standard Model (SM). The decay modes described in this document are all forbidden at the tree level in the SM and are only mediated by loop diagrams. Beyond-SM (BSM) contributions are in general possible at tree level in some models or can contribute to the loops, with an effect on the amplitude of the processes and in other observables. For those decay modes the smallness of the branching ratio (BR) by itself contribute also to make the new physics (NP) contribution evident.

The two Tevatron experiments, CDF[1] and DØ[2], benefit of the large heavy-flavor production cross-section for $p\bar{p}$ collisions at $\sqrt{s} = 1.96\,\text{TeV}$. These conditions make the experiments competitive with the B-factories results on the B^0 and $B^{\pm}$ modes, with the unique opportunity at the same time to investigate the rare decays of the B_s^0 or other b-hadrons. The decay modes in this document involves both leptonic final state, with the $B_{(s)}^0 \to \mu^+\mu^-$ and $B^{0(+)} \to h\mu^+\mu^-$, and purely hadronic mode as the $B_s^0 \to \phi\phi$, giving a further example of the richness of the B-physics programs at the two experiments.

2. $B_s^0 \to \phi\phi$ branching ratio and polarization

The $B_s^0 \to \phi\phi$ decay mode in the SM is dominated by the contribution coming from the penguin diagram, indeed suppressed in the SM. In the recent years the penguin mediated processes have gathered some attention due to discrepancies found between SM prediction and data at B-factories. Further more the $B \to VV$ can be used to measure the $\sin(2\beta_s)$. The CDF experiment observed this decay mode for the first time in 2005, with a BR of $\mathcal{B}\left(B_s^0 \to \phi\phi\right) = [1.4 \pm 0.6 \pm 0.6] \times 10^{-5}$, based on $180\,\text{pb}^{-1}$[3].

The current update is based on a sample of $2.9\,\text{fb}^{-1}$. The online selection is made possible by two dedicated hardware systems XFT[4] and SVT[5]. These two systems, at the first ad second level of the trigger, are able to reconstruct the track parameters with high precision in about $20\,\mu s$; in particular SVT uses the silicon information and allows to recognize events with tracks coming from a displaced vertex and with helix parameters compatible with a B-hadron decay.

The trigger selection used at the Level-2 requires events having two tracks with $p_T \geq 2$ GeV/c and $120\ \mu\text{m} \leq d_0 \leq 1.0$ mm. The two trigger tracks must have an opening angle $2^\circ \leq |\Delta\theta| \leq 90^\circ$ in the transverse plane. Other cuts on the track momenta are applied to further suppress the rate and changes according the instantaneous luminosity. The selection at Level-3 confirms the previous cuts and requires a transverse decay length $L_{xy} \geq 200\,\mu\text{m}$, where the distance is corrected by the beamline position.

The analysis cuts are optimized to maximize the standard figure of merit $F = S/\sqrt{S+B}$,

where S (B) represents the number of signal (background) events. The background is selected from the sidebands, while the signal is simulated using the CDF detailed Montecarlo (MC). As reference mode for the BR, and control sample for the angular analysis, the $B_s^0 \to J/\psi\phi$ is chosen. The reference mode selection is performed using the same trigger selection, the events in common with the di-muon trigger selection used in another analysis about $B_s^0 \to J/\psi\phi$[6] are vetoed to have a completely independent sample in order to check the results.

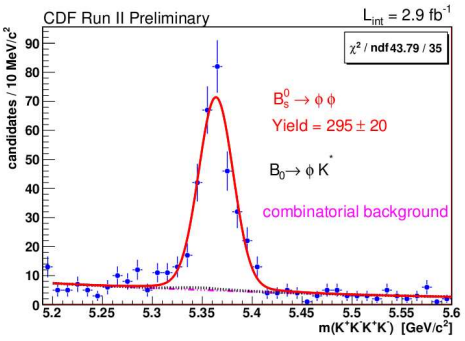

Figure 1. The plot shows the project for the ML fit used to extract the $B_s^0 \to \phi\phi$ BR.

For the BR measurement the selected events are fitted using an unbinned maximum likelihood (ML) fit on invariant mass of the four kaons, with a model composed by two gaussians for the signal peak, a peaking background to account for the $B^0 \to \phi K^\star$ contribution, and a combinatorial background. From the fit results the number of signal events is 295 ± 20, that correcting for the relative efficiency and using the world average value for $\mathcal{B}(B_s^0 \to J/\psi\phi)$ give[7]:

$$\mathcal{B}(B_s^0 \to \phi\phi) = [2.40 \pm 0.21 \pm 0.86] \times 10^{-5}$$

Performing the fit with the addition of three angles, in the so called helicity reference frame, it is possible to disentangle the CP even and odds components. The fit method was cross

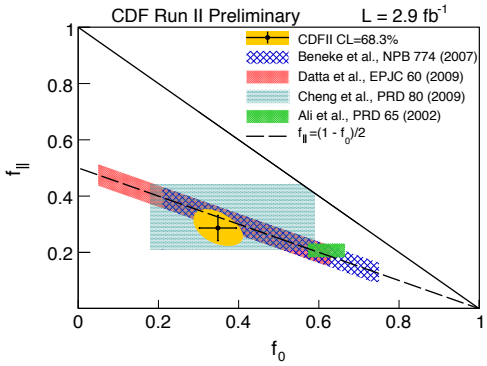

Figure 2. The figure shows the comparison between the CDF measurement and few theoretical prediction.

checked with the $B_s^0 \to J/\psi\phi$ mode, obtaining results compatible with the independent sample used in the $\sin(2\beta_s)$ analysis[6]. The angular analysis here is time integrated, using the values $1/\Gamma_L = 1.408^{+0.033}_{-0.030}$ ps, $1/\Gamma_H = 1.543^{+0.058}_{-0.060}$ ps and the $\Delta\Gamma_s = 0.062^{+0.034}_{-0.037}\,\mathrm{ps}^{-1}$, ϕ_s is set to 0. In the fit the flavor tagging is not used so it is not possible to separate B_s^0 from $\bar{B}_s^0$.

In the angular analysis the effect of the trigger acceptance on angular distribution of the CP-even and CP-odd modes are taken into account using the CDF MC.

The angular analysis allowed to separate the longitudinal and transverse contribution, with a result of $f_L = 0.348 \pm 0.041 \pm 0.021$ and $f_T = 0.652 \pm 0.041 \pm 0.021$[8]. The fig. 2 shows a comparison between the experimental results and some predictions obtained using particular models. The comparison with the theoretical predictions shows a reasonable agreement with some models.

3. $B \to h\mu^+\mu^-$ analysis

The Flavor Changing Neutral Current (FCNC) transition $b \to sl^+l^-$ in the SM is possible in penguin and box diagrams. The CDF was performed on three different modes: $B^0 \to K^{\star 0}\mu^+\mu^-$, $B^+ \to K^+\mu^+\mu^-$, and $B_s^0 \to \phi\mu^+\mu^-$. The modes

involving B^+ and B^0 modes were already observed and studied at the B-Factories, the third mode was never observed before and only an upper limit to its BR exists[12,13].

The most recent CDF analysis uses $4.4\,\mathrm{fb}^{-1}$ of data. The trigger selection requires the identification of two charged muons, with opposite charge, in the region with $|\eta| \leq 1$ and transverse momentum $p_T > 1.5\,\mathrm{GeV/c}$ or $p_T > 2.0\,\mathrm{GeV/c}$ according the trigger condition. Other refinements on the selection are applied to keep the trigger rate under control. The kaon identification relies on the possibility to measure the energy deposited in the tracking chamber and the time-of-flight, the muon identification add the information coming from the muon chambers combined in an likelihood.

The BR measurement is performed selecting for each $B_q \to h\mu^+\mu^-$ the $B_q \to hJ/\psi$ mode as reference, where q stands for u, d, or s quark and h for K^+, $K^\star$, or ϕ meson. The cuts are optimized in two steps: the first optimization step selects the cuts to have the best significance on the reference mode, in this first step the cuts are just rectangular cuts, this is *loose* selection; in the second step the selection is chosen to have the best significance on the signal modes, here an artificial neural network output variable is used, this is the *NN* selection. In the final optimization there is a small difference between modes already observed and the $B_s^0 \to \phi\mu^+\mu^-$: the B^+ and B^0 mode were optimized to obtain the best significance, maximizing the figure of merit $S/\sqrt{S+B}$, for B_s^0 mode was instead used the figure of merit $S/(5/2+\sqrt{B})$ because the mode wasn't observed before and the aim was to obtain a statistical significance of 5σ.

The final BR indeed can be evaluated using the general formula:

$$\frac{\mathcal{B}(sgn)}{\mathcal{B}(ref)} = \frac{N_{sgn}^{NN}}{N_{ref}^{L}} \frac{\epsilon_{ref}^{L}}{\epsilon_{sgn}^{L}} \frac{1}{\epsilon_{sgn}^{NN}} \times \mathcal{B}\left(J/\psi \to \mu^+\mu^-\right)$$

where $N_{sgn(bkg)}^{NN(L)}$ is the number of events for the signal (reference) after NN (loose) selection, $\epsilon_{sgn(ref)}^{L}$ is the signal (reference) efficiency for the loose cuts, and ϵ_{sgn}^{NN} is the signal efficiency after the NN selection.

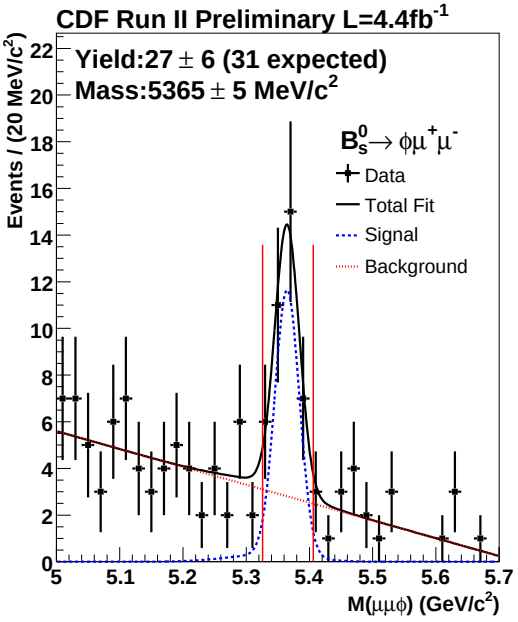

Figure 3. Mass projection for the fit of the $B_s^0 \to \phi\mu^+\mu^-$ decay mode.

The results give:

$$\mathcal{B}\left(B^+ \to K^+\mu^+\mu^-\right) = [0.38 \pm 0.05 \pm 0.03] \times 10^{-6}$$
$$\mathcal{B}\left(B^0 \to K^\star\mu^+\mu^-\right) = [1.06 \pm 0.14 \pm 0.09] \times 10^{-6}$$
$$\mathcal{B}\left(B_s^0 \to \phi\mu^+\mu^-\right) = [1.44 \pm 0.33 \pm 0.46] \times 10^{-6}$$

the statistical signal significance for the modes are: 8.5σ, 9.7σ, and 6.3σ, with the first observation for the $B_s^0 \to \phi\mu^+\mu^-$ mode, fig. 3 show the fit results for the $B_s^0 \to \phi\mu^+\mu^-$ mode.

For the $B^{+(0)} \to K^{+(\star 0)}\mu^+\mu^-$ modes it is also possible to extract other parameters of the decays, related to the kinematic, that are well predicted by the SM. Those parameters are the longitudinal polarization fraction (FL) and the forward-backward asymmetry (AFB).

The AF and K^{*0} FL are extracted from $\cos\theta_\mu$ and $\cos\theta_K$ distributions, respectively, where θ_μ is the helicity angle between μ^+ (μ) direction and the opposite of the B ($\bar{B}$) direction in the dimuon rest-frame, and θ_K is the angle between the kaon direction and the direction opposite to

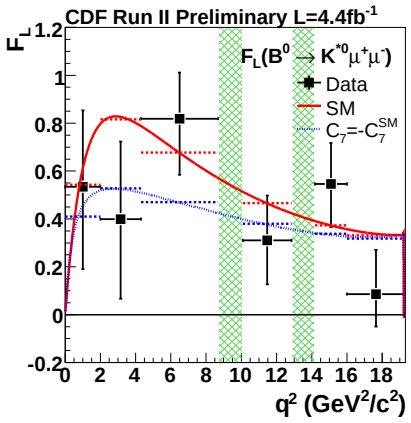

Figure 4. Longitudinal polarization of the $B^0 \to K^\star\mu^+\mu^-$ in bins of di-muon invariant mass. The lines show the SM prediction and a NP model.

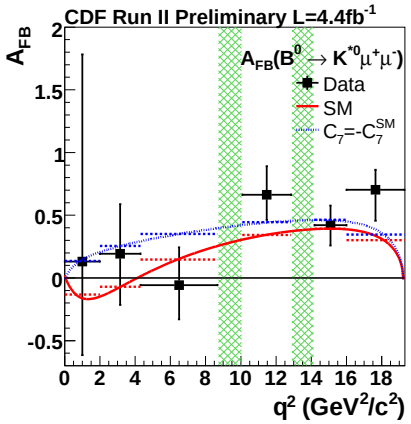

Figure 5. Result for the forward-backward asymmetry for the $B^0 \to K^{\star 0}\mu^+\mu^-$ in 6 bins of di-muon invariant mass. The two bands show the vetoes on the J/ψ and ψ'. The SM (the bottom red curve) and one NP model (the top bottom curve) predictions are compared with the experimental data.

the B meson in the $K^{\star 0}$ rest frame.

The FL parameter is well predicted by the SM as function of the squared di-muon mass q^2. The result is shown in fig. 4 where within the statistical uncertainty the data are in agreement with the model.

For both $B^0 \to K^{\star 0}\mu^+\mu^-$ and $B^+ \to K^+\mu^+\mu^-$, in the reference frame were the two muons decay at rest. the observable $\cos(\theta)$ is defined. The $\cos(\theta)$ is the scalar product between the directions of the μ^+ and B in this particular reference frame. Separating the sample between $\cos(\theta) > 0$ from the $\cos(\theta) < 0$ it is possible to evaluate the so called forward-backward asymmetry:

$$A_{FB}\left(q^2\right) = \frac{N(q^2, \cos(\theta) > 0) - N(q^2, \cos(\theta) < 0)}{N(q^2, \cos(\theta) > 0) + N(q^2, \cos(\theta) < 0)}$$

The value of the asymmetry is predicted in the SM and in many BSM theories as function of the di-muon mass. The fig. 5 shows how the experimental data are in agreement with the SM prediction but also with some of the BSM models[9].

4. $B^0_{(s)} \to \mu^+\mu^-$ search

The $B^0_{(s)} \to \mu^+\mu^-$ is considered one of the golden channels to test the SM prediction in the flavor sector. This because the purely leptonic final state limit the uncertainty due to hadronic form factors. Moreover the contribution of the NP in many models can be precisely computed. In this scenario the SM prediction for the BR is $\mathcal{B}\left(B^0_s \to \mu^+\mu^-\right) = [3.6 \pm 0.4] \times 10^{-9}$[10], with a further suppression $\left(V_{td}/V_{ts}\right)^2 \simeq 0.04$ for the $B^0 \to \mu^+\mu^-$.

Those decay modes are also favorite from the experimental point of view, because the di-muon final states is a very clean signature. The search is performed by both CDF and DØ with a very similar selection, the main differences are the muon coverage and mass resolution: CDF has a good coverage up to $|\eta| < 1$ with a mass resolution of about 25 MeV/c^2, DØ coverages is up to $|\eta| < 3$ with a mass resolution about 100 MeV/c^2.

The data selection and the analysis technique

are similar in both experiments: the selection is based on a search for a di-muon candidate, with a multivariate classifier to identify $B^0_{(s)} \to \mu^+\mu^-$candidate. The CDF analysis uses an artificial neural network (ANN), while DØ uses a Bayesian neural network (BNN). The classifier uses as input variable the muon momenta, the candidate isolation, the decay length and other kinematic variables, with the exclusion of the dimuon mass. The background training sample is taken from the sidebands while the signal sample is obtained generating $B^0_s \to \mu^+\mu^-$ events with an event generator and processing the events through the experiment's MC simulation. The CDF experiment, due to the better mass resolution, can also perform a direct search for the $B^0 \to \mu^+\mu^-$ decay mode.

The background sources are semileptonic decays of b and c-hadron, in particular there are two sources: one is composed by the double semileptonic decays, like $B\bar{B} \to \mu^+\mu^- X$ or $D\bar{D} \to \mu^+\mu^- X$, the other is composed by sequential semileptonic decays, like $B \to \mu^+\nu\bar{D}, \bar{D} \to \mu^-\bar{n}uX$. An additional source to the previous is when there is a real muon and fake muon from misidentification of pions and kaons. A peaking background comes from the hadronic decays $B \to h^+h'^-$, when both hadrons are faked as muons, but this is found to be negligible for the $B^0_s \to \mu^+\mu^-$.

The BR of the decay can is obtained using as reference the $B^+ \to J/\psi K^+$ decay mode using the following formula:

$$\mathcal{B}\big(B^0_s \to \mu^+\mu^-\big) = \frac{N(B^0_s)}{N(B^+)} \cdot \frac{\epsilon_{B^+}}{\epsilon_{B^0_s}} \cdot \frac{f_u}{f_s} \cdot \mathcal{B}\big(B^+\big)$$

where $N(B^0_s)$ and $\epsilon_{B^0_s}$ are the yield and the efficiency for the signal, $N(B^+)$ and ϵ_{B^+} are the number of B^+ decay mode and the analysis efficiency. For the fragmentation function DØ chooses the PDG 2006 value $f_u/f_s = 3.86 \pm 0.59$ to better compare with the previous measurements. The limit is evaluated using the pseudo-frequentist confidence level approach (CL_s)[14]. DØ based on 6.1 fb^{-1} doesn't observe any excess, setting an upper limit to $\mathcal{B}\big(B^0_s \to \mu^+\mu^-\big) < 5.1 \times 10^{-8}$ at the 95% C.L. showed in fig. 6 [15]. This is consistent with the CDF preliminary result published in 2009, based on 3.7 fb^{-1} was already presented at conference, with the limits $\mathcal{B}\big(B^0_s \to \mu^+\mu^-\big) < 4.3 \times 10^{-8}$ at 95% C.L.[16].

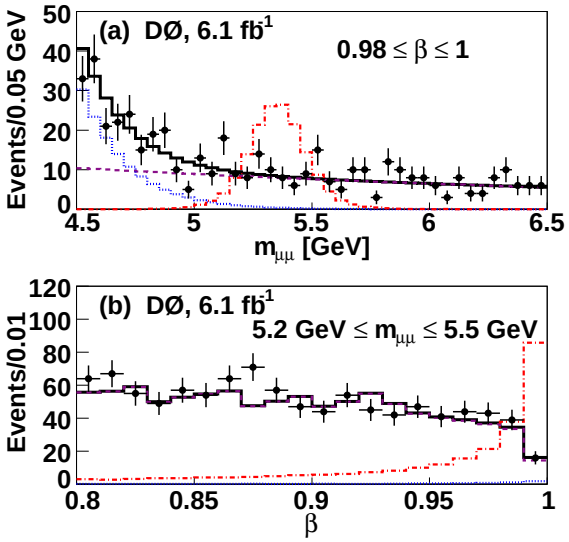

Figure 6. The plots show the mass projection from the DØ analysis for the most significant bin for the BNN output (on the top), and for the BNN in the B^0_s mass window (on the bottom).

5. Conclusions

The Tevatron experiments are giving a very important contribution in the study of B rare decays, helping to define how the new physics could appear in this field. The CDF experiment reports a new results for the the $B^0_s \to \phi\phi$ mode, with the first determination of the polarization amplitudes, a measurement on the $B^{0(+)} \to h\mu^+\mu^-$ modes with a precision similar to the one obtained at the B-factories on the same modes, plus the first observation of the $B^0_s \to \phi\mu^+\mu^-$. The DØ experiment reports an update on the search of the $B^0_s \to \mu^+\mu^-$ decay. No events are found, the limit on this mode is compatible with the expectation and the recent CDF measurement.

The presented results can be further improved in the middle term because they are generally

based on a part of the total 10 fb^{-1} per experiment that the Tevatron is expected to provide.

REFERENCES

1. The CDFII Detector Technical Design Report, Fermilab-Pub-96/390-E; D. Acosta, et al., Phys. Rev. D 71, 032001 (2005).
2. D0 Collaboration, V. M. Abazov et al., Nucl. Instrum. Methods in Phys. Res. A 565, 463 (2006).
3. D.Acosta et al. (CDF Collaboration),Phys. Rev. Lett. 95, 031801, 2005.
4. E. J. Thomson et al. Online Track Processor for the CDF Upgrade. IEEE Trans. Nucl. Sci., 49, 2002.
5. W. Ashmanskas, et al., Nucl. Instrum. Methods A 518, 532 (2004).
6. T. Aaltonen *et al.* [CDF Collaboration], Phys. Rev. Lett. **100** (2008) 161802 [arXiv:0712.2397 [hep-ex]].
7. CDF Collaboration, CDF-Note 10064 (2010).
8. CDF Collaboration, CDF-Note 10120(2010).
9. CDF Collboration, CDF-Note 10047 (2009).
10. A. J. Buras, Prog. Theor. Phys. 122, 145 (2009).
11. W.-M. Yao et al., Journal of Physics G 33, 1 (2006).
12. T. Aaltonen et al. (CDF), Phys. Rev. D79, 011104 (2009), arXiv:0804.3908.
13. V. M. Abazov et al. (D0), Phys. Rev. D74, 031107 (2006), arXiv:hep-ex/0604015.
14. T. Junk, Nucl. Instrum. Methods in Phys. Res. A 434, 435 (1999).
15. DØ Collaboration, FERMILAB-PUB-10-202-E (2010).
16. CDF Collaboration, CDF Note 9892 (2009), arXiv:1006.3469 [hep-ex].